Low rank perturbations and the spectral statistics of pseudointegrable billiards

Thomas Gorin
*Theoretische Quantendynamik, Universität Freiburg, Hermann-Herder-Str 3, D-79104 Freiburg**

Jan Wiersig
Institut für Theoretische Physik, Universität Bremen, Kufsteiner Str., D-28359 Bremen, Germany
(Dated: February 8, 2008)

We present an efficient method to solve Schrödinger's equation for perturbations of low rank. In particular, the method allows to calculate the level counting function with very little numerical effort. To illustrate the power of the method, we calculate the number variance for two pseudointegrable quantum billiards: the barrier billiard and the right triangle billiard (smallest angle $\pi/5$). In this way, we obtain precise estimates for the level compressibility in the semiclassical (high energy) limit. In both cases, our results confirm recent theoretical predictions, based on periodic orbit summation.

PACS numbers: 02.70.-c, 03.65.Ge, 05.45.Mt

arXiv:nlin/0303034v2 [nlin.CD] 18 Mar 2003

Consider the stationary Schrödinger equation for a quantum system, which can be described by a Hamiltonian $H = H_0 + W$ with the following properties: The operators H and H_0 have discrete spectra, the eigenbasis of H_0 is known, and the perturbation W is non-negative (or non-positive) and of low rank. Then, our method allows to evaluate the level counting function at arbitrary energies, by solving an eigenvalue problem of the dimension which is equal to the rank of the perturbation. At first sight, the requirements seem rather restrictive, but in fact, there are a number of problems which can comply with them. For example, one may think of a few particle system with some kind of short range residual interaction.

To illustrate how the method works, we choose two examples of a different type, the so called "barrier billiard" [1], and the right triangle billiard [2] with smallest angle $\pi/5$. Both examples are twodimensional, pseudointegrable polygon billiards [2, 3]. While pseudointegrable systems have enough constants of motion to assure local integrability, singularities in the Hamiltonian flow allow invariant surfaces with genus larger than one.

In the spirit of quantum-classical correspondence, there have been numerous efforts to study the implications of pseudointegrability on the quantum spectrum [3, 4, 5, 6, 7, 8]. In Refs. [5, 9] it is conjectured that the statistical properties of pseudointegrable billiards is intermediate between Poisson statistics, typically related to integrable systems [10], and the eigenvalue statistics of the Gaussian orthogonal ensemble [11], related to fully chaotic (time reversal invariant) systems. The so called "intermediate statistics" has also been found in disordered, mesoscopic systems at the metal-insulator transition [12], for systems with interacting electrons [13], and for incommensurate double-walled carbon nanotubes [14].

A suitable measure for intermediate statistics is the level compressibility $\chi = \lim_{L\to\infty} \Sigma^2(L)/L$, where $\Sigma^2(L)$ is the number variance [11] for energy intervals of length L (measured in units of the average level spacing). Note that χ coincides with the value of the spectral two-point formfactor in the limit of small times. Recently, analytical results for χ became available for a certain class of right triangle billiards (including our example) [15], as well as for the barrier billiard [8]. However, the convergence to the semiclassical limit is so slow, that numerical studies could not confirm those results with the desirable clarity. For example in the case of the barrier billiard one obtains $\chi \approx 0.34$ in the region between level number 400 000 and 420 000, while the semiclassical prediction is $\chi = 1/2$ [8].

As we will show below, our method is almost ideally suited for the calculation of the number variance for large values for L. Therefore, we are able to calculate the level compressibility at much higher energies and with better statistics. In the case of the barrier billiard, for example, we calculate number variances in the region of absolute level number $\mathcal{N} > 1.6 * 10^7$ within an energy range which contains about 10^5 levels.

Here we can only sketch the general method. A detailed presentation will be published elsewhere, and an early implementation can be found in Ref. [7]. Assume, that the Hamiltonian H can be approximated by a projection on an appropriately chosen N-dimensional Hilbertspace, $N < \infty$. Furthermore, assume that its matrix representation is of the following form:

$$H = H_0 + \eta\, V\, V^\dagger\,. \tag{1}$$

Here V is a $N\times M$-matrix with mutually orthogonal column vectors, $M < N$, and η is a positive parameter. Such a representation can be obtained, for instance, by diagonalizing a non-negative perturbation of small rank M. Then, in general, the spectrum of H consists of a trivial component S_0, contained in the spectrum of H_0, and a non-trivial component S_1, which is disjoint. The

*Electronic address: Thomas.Gorin@physik.uni-freiburg.de

eigenvalues in S_1 are roots of the secular equation

$$\det[1-\eta K(E)] = 0\ , \quad K(E) = V^\dagger\ \frac{1}{E-H_0}\ V\ , \qquad (2)$$

where the matrix $K(E)$ is of dimension M [7]. Eq. (2) can be considered as an eigenvalue equation $K(E)\,\vec{x} = \delta\,\vec{x}$, where one of the eigenvalues must be equal to η^{-1}.

Differentiating $K(E)$ with respect to the energy gives a negative definite matrix. This shows that the eigenvalues of $K(E)$ are monotonously decreasing with energy. The eigenvalues of H_0 coincide with the positions of the poles of $K(E)$. Therefore, each time the energy moves across a pole, a new eigenvalue of $K(E)$ appears at $+\infty$. The eigenvalue decreases with energy, until it reaches the value $1/\eta$. At this point the secular equation (2) has a root. Beyond this point, the eigenvalue continues to decrease, until it disappears at $-\infty$. This behavior gives rise to the following *sum rule*: Let $n_0(n_1)$ denote the number of eigenvalues of $K(E)$, larger than $1/\eta$, at $E = E_0(E_1)$, and let N_p denote the number of poles and N_r the number of roots of $\det[K(E)]$ in the interval (E_0, E_1). Then it holds:

$$n_0 + N_p - N_r = n_1\ . \qquad (3)$$

At the one hand, this relation can be used to bracket the eigenvalues in S_1, before using a standard root searching algorithm to obtain the desired accuracy. In this case, Eq. (3) assures, that no eigenvalues are overlooked. On the other hand, in order to study the long range correlations, it can be sufficient to calculate the level counting function at the points of an equi-distant grid (in units of the average level spacing) grid in the energy region of interest. If $L_{\rm st}$ denotes the stepsize, one can obtain the number variance at integer multiples of $L_{\rm st}$ from this data.

To calculate the spectrum of the barrier billiard [8], we choose as H_0 the Hamiltonian of a rectangle billiard with sides of length a and b. With the origin of a Cartesian coordinate system fixed at one of the corners, the normalized eigenfunctions are

$$\Psi_{mn}(x,y) = 2(ab)^{-1/2}\ \sin(\pi m x/a)\ \sin(\pi n y/b)\ , \qquad (4)$$

while $\varepsilon_{mn} = [(m/a)^2 + (n/b)^2]\,\pi^2/2$ are the corresponding eigenvalues. We use units, in which the mass and Planck's constant $\hbar$ are both equal to one. The perturbation consists of an additional boundary segment inside the billiard, connecting the points $(a_0, 0)$ and (a_0, c). It is modeled by a potential well with delta shaped profile:

$$H = H_0 + \eta W\ , \quad W = (a/2)\ \delta(x-a_0)\ \theta(c-y), \qquad (5)$$

where $\delta(x)$ is the usual δ-function, and $\theta(y)$ is the unit step function. The prefactor $a/2$ is included for convenience. As η increases from 0 to ∞, the spectrum of H changes from the spectrum of the rectangle billiard to the spectrum of the barrier billiard.

In what follows we set $a_0 = a/2, c = b/2$, where $a = 2\pi^{3/2}/3$ and $b = 6/\pi^{1/2}$. In this way, we obtain the same spectrum as in Ref. [8]. In this case the trivial component S_0 of the spectrum corresponds to states Ψ_{mn} with a node line at $x = a/2$. In order to obtain the non-trivial component alone, we require the eigenstates to be reflection symmetric with respect to that line. In other words, we consider the spectrum of a new rectangle billiard with sides $a/2$ and b, which has Dirichlet boundaries everywhere, except for the boundary segment between the points $(a/2, b/2)$ and $(a/2, b)$ where it has a von Neumann boundary.

To obtain the decomposition $W = V\,V^T$, we calculate all eigenvectors of W which correspond to nonzero eigenvalues. This is rather simple because W is separable in the x- and y-modes of the eigenfunctions of H_0:

$$V^{(\alpha)}_{mn} = s(m)\ \tilde{A}^{(\alpha)}_n \qquad s(m) = \sin(\pi m/2) \qquad (6)$$

$$\tilde{A}^{(\alpha)}_{2n} = \frac{\delta_{n\alpha}}{\sqrt{2}} \qquad \tilde{A}^{(\alpha)}_{2n-1} = \frac{\sqrt{2}\,\alpha}{\pi}\ \frac{(-)^{\alpha+n}}{\alpha^2-(n-1/2)^2}\ . \qquad (7)$$

For the matrix elements of $K(E)$ we get:

$$K_{\alpha\beta}(E) = \sum_{mn} \frac{V^{(\alpha)}_{mn}\ V^{(\beta)}_{mn}}{E-\varepsilon_{mn}} = \sum_{mn} \tilde{A}^{(\alpha)}_n\ \tilde{A}^{(\beta)}_n\ \frac{s(m)^2}{E-\varepsilon_{mn}}\ . \qquad (8)$$

In the limit $m \to \infty$, we can evaluate the sum over m analytically:

$$K_{\alpha\beta}(E) = \frac{a^2}{2\pi} \sum_n \tilde{A}^{(\alpha)}_n\ \tilde{A}^{(\beta)}_n\ G_n(E)\ , \qquad (9)$$

with $G_n(E) = -\tan(\pi z_n/2)/z_n$. Here, z_n is the effective quantum number for H_0 at given energy E, *i.e.* $(z_n\pi/a)^2 + (n\pi/b)^2 = 2E$. Note that $G_n(E)$ remains real, even for imaginary z_n. Introducing the orthogonal matrix $A_{nm} = \sqrt{2}\,\tilde{A}^{(n)}_{2m-1}$ we may write:

$$K(E) = \frac{a^2}{4\pi}(A\ G^{\rm odd}\ A^T + G^{\rm even})\ , \qquad (10)$$

with $G^{\rm odd} = {\rm diag}[G_{2n-1}(E)]$, and $G^{\rm even} = {\rm diag}[G_{2n}(E)]$. Multiplying Eq. (10) from left and/or right by A^T and/or A, one can construct additional variants: $L = A^T\,K$, $K' = A^T\,K\,A$, and $M = K\,A$. Any one can be used in the secular equation (2) to find the eigenvalues of the barrier billiard. However, the matrices $K(E)$ and $K'(E)$ are real and symmetric, and hence easy to diagonalize. For the analysis below, we use $K'(E)$, because it turned out that the numerical procedure converges faster in this case. In Ref. [8] the non-symmetric matrix $M(E)$ has been used, instead.

In what follows, we aim at a precise, numerical estimate for the level compressibility, which can be compared to the analytical results obtained in [8, 9]. To this end, we compute the level counting function on a finite grid $\mathcal{N}_0, L_{\rm tot}, L_{\rm st}$ of consecutive intervals of length $L_{\rm st}$, starting at $\mathcal{N}_0$ and ending at $\mathcal{N}_0 + L_{\rm tot}$. The grid is defined on

	(A)	(B)	(C)	(D)
$\mathcal{N}_0 =$	$8 * 10^5$	$2 * 10^6$	$8 * 10^6$	$1.6 * 10^7$
$L_{\rm tot} =$	10^5	$1.4 * 10^5$	10^5	10^5

TABLE I: Data sets for the barrier billiard.

the unfolded energy axis, where the average level spacing is equal to one. It is mapped onto the physical energy axis, by inverting the Weyl law [16]:

$$\mathcal{N}(E) = \frac{ab}{4\pi}\, E - \frac{a+b}{4\pi}\, \sqrt{2E} + \frac{1}{16}\ . \qquad (11)$$

We count the number of levels in each interval, using the sum rule, Eq. (3). The data sets, listed in Tab. I, are produced in this way. Finally, they are used, to calculate the number variance $\Sigma^2(L)$ at integer multiples of $L_{\rm st} = 10$. To get an idea of the efficiency of the method, note that it took about twenty days on a PC running at 1.7 GHz, to produce the data set (D). The dimension of the matrices, to be diagonalized, was approximately 3700.

According to Ref. [17], the number variance $\Sigma^2(L)$ saturates at $L \approx L_{\rm max}$, which is related to the inverse period of the shortest (non-diffractive) periodic orbit. For our barrier billiard

$$L_{\rm max} = \sqrt{2\pi\, \mathcal{N}_0\ b/a} = \sqrt{18\, \mathcal{N}_0/\pi}\ . \qquad (12)$$

At large $L \gg 1$, the ratio $\Sigma^2(L)/L$ is constant at first, but it starts to decrease, when L approaches $L_{\rm max}$. Therefore, we may expect that a plot: $\Sigma^2(L)/L$ versus $L/L_{\rm max}$ depends only weakly on $L_{\rm max}$, *i.e.* the energy range $\mathcal{N}_0$. We call this function the *scaled number variance*:

$$g(x) = \Sigma^2(L_{\rm max}\, x)/(L_{\rm max}\, x)\ . \qquad (13)$$

In theory it is expected that in a given energy region, the ratio $\Sigma^2(L)/L$ approaches its limit value quite quickly; for instance, $L \approx 10$ seems to be sufficient, to obtain accurate results. The semiclassical limit $\mathcal{N}_0 \to \infty$ is the really difficult one. In this limit the level compressibility must be estimated by extrapolation: $\chi = \lim_{x\to 0} g(x)$.

Fig. 1 shows the scaled number variance for the data sets given in Tab. I. For the error bars, we estimated that the relative error is approximately equal to $1.6\,\sqrt{L/L_{\rm tot}}$. In order to check this, we computed the variance of the distribution of different partial averages, fitting them with a normal distribution. Note that $L_{\rm tot}/L$ gives the number of independent level counts, in the energy range considered. Fig. 1 explains the discrepancy between the numerical estimate for the level compressibility obtained in Ref. [8], and the theoretical expectation. In the region $x > 0.01$ the scaled number variance looks perfectly linear. Hence, in the absence of data points with $x < 0.01$, one is lead to assume that the linear behavior continues down to the point $x = 0$. However, for $x < 0.01$, the slope changes drastically, and a second linear regime appears. Then indeed, the scaled number variance $g(x)$ approaches the theoretical prediction $\chi = 1/2$ as $x \to 0$. In order

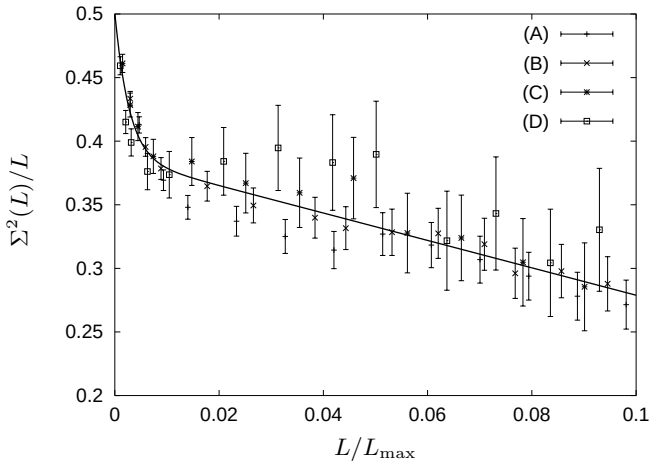

FIG. 1: The scaled number variance $\Sigma^2(L)/L$ versus $x = L/L_{\rm max}$, for the four data sets given in Tab. I. For clarity, only some of the data points are plotted. The thick solid line gives the fit function $g(x)$ with parameters as given in Eq. (15).

to put our findings on a quantitative basis, consider the following phenomenological parametrization:

$$g(x) = a_2 - a_1 x + (a_0 - a_2)\exp(-a_3 x)\ . \qquad (14)$$

Its form is such that $a_0 = g(0)$ gives the best estimate for the level compressibility in the semiclassical limit. At the same time, both linear regimes are reproduced. By consequence, a_2 would be the estimate for the level compressibility, in the absence of data points with $x < 0.01$. For the fit, all data sets in Tab. I are taken into account, excluding only those data points, for which $x > 0.2$. Beyond this point (which is outside the interval shown in Fig. 1) the parametrization (14) breaks down. Using the nonlinear least squares Marquardt-Levenberg algorithm [18], we obtain the following estimates for the fit-parameters:

$$\begin{aligned} a_0 &= 0.5008(91) \qquad a_1 = 1.077(18) \\ a_2 &= 0.3866(17) \qquad a_3 = 364(39) \end{aligned} \qquad (15)$$

with a reduced chi-square value of $\chi^2_{\rm fit}/f \approx 0.54$ (the number of degrees of freedom is $f = 305$).

With a_0, we have finally obtained a precise numerical estimate for the level compressibility in the semiclassical limit. It agrees within a relative error of roughly two percents with the theoretical result $\chi = 1/2$. In addition, the moderate value for $\chi^2_{\rm fit}$ is quite remarkable. It gives some support to the assumption that within the statistical error, the scaled number variance is independent of the energy region (as long as $x \lesssim 0.2$).

In what follows, we repeat the numerical analysis for the $\pi/5$-right triangle billiard. In this case the length scale $L_{\rm max}$, for the saturation of the number variance, is about 2.6 times smaller than for the barrier billiard, *i.e.*

$$L_{\rm max} = \sqrt{2\pi\, \mathcal{N}_0/(8\, \sin 2\alpha)} \qquad \alpha = \pi/5\ . \qquad (16)$$

	(T1)	(T2)	(T3)
$\mathcal{N}_0 =$	$4*10^5$	10^6	$4*10^6$
$L_{\rm tot} =$	$4*10^4$	10^5	10^5

TABLE II: Data sets for the right triangle billiard ($\alpha = \pi/5$).

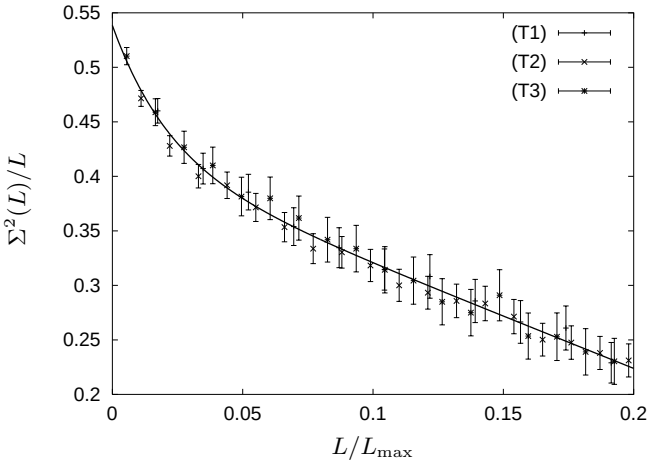

FIG. 2: The scaled number variance for the data sets in Tab. II. Only a subset of the data points is plotted. The solid line gives the fit $g(x)$ with parameters as given in Eq. (17).

We calculated three data sets in different energy regions, as listed in Tab. II. The stepsize was again $L_{\rm st} = 10$. With all data sets, we fit the scaled number variance $g(x)$ using the parametrization (14), excluding as before all data points with $x > 0.2$. The resulting estimates are:

$$\begin{aligned} a_0 &= 0.5385(57) \qquad a_1 = 0.958(37) \\ a_2 &= 0.4154(54) \qquad a_3 = 46.2(5.4) \end{aligned} \tag{17}$$

with a reduced chi-square value of $\chi^2_{\rm fit}/f \approx 0.20$ ($f = 61$). The numerical results for $g(x)$, and the fit with Eq. (14), are plotted in Fig. 2. For the error bars, we have checked, that the same approximation holds as in the case of the barrier billiard. The absolute errors are smaller here, because the data sets are taken at lower energy ranges. As in Fig. 1, we find two different linear regimes, with a transition which occurs somewhat earlier, at $x \approx 0.04$. The overall change in the graph is less dramatic because the slope at $x < 0.04$ is much smaller in magnitude. Though the agreement of the extrapolated value for $g(0)$ with the theoretical expectation $\chi = 5/9$ [15] is not perfect, our estimate is quite close to it. Note that the error estimates for the parameters $a_0, \ldots, a_3$ are also based on statistical data. In particular in the case of a_0, there are only relatively few relevant data points. This leads to rather large uncertainties. In general the data points fluctuate much less than in the case of the barrier billiard, as can be read off from the smaller value for $\chi^2_{\rm fit}/f$.

We advanced the technique, recently proposed in [7], to solve the Schrödinger equation for perturbations of low rank. We realized that due to a special *sum rule*, one can obtain the level counting function with very little numerical effort. Systems involving short range interactions may be good candidates for future applications. In this letter, we considered two pseudointegrable billiards: the barrier billiard and the $\pi/5$-right triangle billiard. In spite of their apparent simplicity, the spectral statistics, a corner stone in quantum-classical correspondence, is only hardly understood. We performed extensive numerical calculations for the number variance $\Sigma^2(L), L \gg 1$ in energy regions up to $\mathcal{N} \geq 1.6*10^7$ (for the barrier billiard) and $\mathcal{N} \geq 4.*10^6$ (for the right triangle billiard). With the help of the *scaled number variance*, we obtained very precise estimates for the level compressibility, which largely confirm previously obtained analytical results.

T.G. thanks L. Kaplan and T. Papenbrock for stimulating discussions at the Centro Internacional de Ciencas in Cuernavaca, Mexico, and the EU Human Potential Program contract HPRN-CT-2000-00156 for financial support.

[1] J. H. Hannay and R. J. McCraw, J. Phys. A **23**, 887 (1990).
[2] E. Gutkin, Physica **19D**, 311 (1986); J. Stat. Phys. **83**, 7 (1996).
[3] P. J. Richens and M. V. Berry, Physica D **2**, 495 (1981).
[4] B. Grémaud and S. R. Jain, J. Phys. A **31**, L637 (1998).
[5] E. B. Bogomolny, U. Gerland, and C. Schmit, Phys. Rev. E **59**, R1315 (1999).
[6] G. Casati and T. Prosen, unpublished (1999).
[7] T. Gorin, J. Phys. A **34**, 8281 (2001).
[8] J. Wiersig, Phys. Rev. E **65**, 046217 (2002).
[9] E. Bogomolny, U. Gerland, and C. Schmit, Eur. Phys. J. B **19**, 121 (2001).
[10] M. V. Berry and M. Tabor, Proc. R. Soc. Lond. A **356**, 375 (1977).
[11] M. Mehta, *Random matrices and the statistical theory of energy levels* (Academic Press, New York, 1991).
[12] B. Shklovskii *et al.*, Phys. Rev. B **47**, 11487 (1993).
[13] X. Waintal, D. Weinmann, and J. Pichard, Eur. Phys. J. B **7**, 451 (1999).
[14] K.-H. Ahn, Y. H. Kim, J. Wiersig, and K. J. Chang, Phys. Rev. Lett. **90**, 026601 (2003).
[15] E. Bogomolny, O. Giraud, and C. Schmit, Commun. Math. Phys. **222**, 327 (2001).
[16] M. Brack and R. K. Bhaduri, *Semiclassical physics* (Addison Wesley, New York, 1997).
[17] M. V. Berry, Proc. R. Soc. Lond. A **400**, 229 (1985).
[18] Gnuplot 3.7, patchlevel 1 (1999).